Journal of Thermal Analysis and Calorimetry, Vol. 69 (2002) 773–783

HEAT CAPACITY CALORIMETRY
Detection of low frequency modes in solids and an application to negative thermal expansion materials

J. Boerio-Goates[*]*, R. Stevens, B. Lang and B. F. Woodfield*

Department of Chemistry and Biochemistry, Brigham Young University, Provo, Utah 84602, USA

Abstract

Experimental heat capacity measurements of α-ZrW_2O_8, and zeolitic polymorphs of SiO_2, BEA and MFI, have been made from 0.6 to 400 K. Measurements on β-$ZrMo_2O_8$ have been made from 8 to 400 K. Analysis of the results yields evidence for very low frequency modes in all four materials. These modes are responsible for negative thermal expansion behavior in α-ZrW_2O_8 and β-$ZrMo_2O_8$. Negative thermal expansion has been observed in some pure SiO_2 zeolites, but no studies have been made to look for it in BEA and MFI. The appearance of low frequency modes in these two zeolites suggests that temperature dependent structural investigations would be worthwhile. These modes are lower in energy than the Boson peak in vitreous silica.

Keywords: Boson peak, heat capacity, negative thermal expansion, specific heat, zeolites

Introduction

The heat capacity (or specific heat) probes the energy states present in a material. Many examples are known. The text by Gopal, while outdated in terms of examples, provides an excellent theoretical introduction to these topics [1].

This paper addresses the ability of heat capacity measurements to obtain semi-quantitative information about the energy and nature of vibrational modes of a solid. These include external modes associated with acoustic and optic phonons that arise from translational motions of the unit cells and internal optic modes associated with vibrations of discrete molecular entities within the unit cell.

Often the true vibrational spectrum is too complicated to be calculated from theoretical principles, or it may be dominated by a few key features. In such cases, the general features of the energy spectrum that can be extracted from analysis of the heat capacity may still be useful. We will present examples taken from two sets of materials that illustrate this point.

We begin with two members of a family that exhibit significant negative thermal expansion, α-ZrW_2O_8 and β-$ZrMo_2O_8$. The α and β forms of ZrW_2O_8 have similar gen-

* Author for correspondence: E-mail: boerio-goates@byu.edu

1418–2874/2002/ $ 5.00

Akadémiai Kiadó, Budapest
Kluwer Academic Publishers, Dordrecht

eral structure. The α form has an ordered arrangement of WO_4 tetrahedra while the β-form has those tetrahedra disordered over two positions and a significant amount of oxygen mobility. In α–ZrW_2O_8, which shows a large negative thermal expansion over an extended temperature range, acoustic vibrations and very low-frequency optic modes have been shown to have negative Gruneisen parameters and thus to be responsible for the NTE effect [2–8]. The first evidence for such low frequency modes came from analysis of the heat capacity [4]. Cubic $ZrMo_2O_8$ has been studied less extensively than its tungstate analogue, but it also exhibits NTE down to low temperatures [9, 10]. It has been synthesized only in the disordered β-form.

We also consider two pure SiO_2 molecular sieves (zeolites). Pure SiO_2 meets the criteria established to date for NTE: rigid units loosely coupled together and two-coordinate oxygen atoms. NTE behavior was predicted for zeolites [11] and has been reported in several zeolitic polymorphs of SiO_2 [12–15]. Heat capacities in the region $10<T/K<400$ have revealed low energy phenomena in these polymorphs [16]. New measurements in the region $0.6<T/K<100$ on purer samples support that conclusion. Plots of the data as C/T^3 *vs*. ln(T/K) show the presence of low frequency modes comparable to those observed in the tungstate and molybdate and lower in energy than what is commonly referred to as the Boson peak in vitreous silica [17]. NTE behavior has not been reported in these two SiO_2 polymorphs. However, to the extent that low frequency modes are required for its presence, one might predict its appearance given the low frequency modes observed in these polymorphs.

Experimental techniques

The heat capacities presented in this paper have been made on two cryogenic calorimeters. The low temperature apparatus is capable of measurements from $0.5<T/K<100$ using a combination of isothermal and semi-adiabatic techniques. A description of a similar apparatus has been published elsewhere [18]. The high temperature apparatus, capable of measurements in the range $5\leq T/K\leq 400$, is an adiabatic calorimeter of the Westrum design. It has been described previously in the literature [19].

The combination of the two apparatus' allows us to measure heat capacities on the same samples over temperature regions in which both cryostats operate optimally. We combine the two sets of experimental results by inspecting the region of overlap and scaling the low-temperature values so that they map smoothly onto the high temperature values. Sample masses are typically 0.2–0.8 g in the low-temperature apparatus and are about 7–15 g in the high-temperature one.

Negative thermal expansion materials

Zirconium tungstate and molybdate

Cubic ZrW_2O_8 has been studied extensively after its unusual NTE behavior was reported [2]. Ramirez and Kowach [4] first demonstrated that the tungstate had a large heat capacity at low temperatures and speculated that the low energy states which

gave rise to the anomalous heat capacity might also be those responsible for the NTE. We have studied a new sample of cubic α-ZrW_2O_8 prepared by Kowach and a sample of cubic β-$ZrMo_2O_8$ that has also been shown to exhibit negative thermal expansion from room temperature. The tungstate was provided as a ceramic pellet, which we broke into small chunks to fit into the calorimeter vessel of the high-temperature cryostat. Those same chunks were fastened to the sample platform of the low-temperature apparatus using Apiezon–N grease. The molybdate was prepared according to the method of Ref. [9] by Lind *et al*. and provided to us as a powder. Soft pellets of the powder were prepared to facilitate thermal equilibration in the high-temperature calorimeter. Pelletizing pressures were kept well below 0.7 GPa, where β-$ZrMo_2O_8$ has been reported to undergo a phase transition pressure [20].

We have recently measured the heat capacity of the grease in the low-temperature apparatus to ensure an accurate correction for its heat capacity in these experiments.

Figure 1 shows the heat capacity of the cubic zirconium tungstate and molybdate as measured at BYU on the high temperature apparatus. Included in Fig. 1 are three other sets of results reported in the literature for α-ZrW_2O_8. Those of Ramirez and Kowach [4] were obtained using a semi-adiabatic heat-pulse technique from 1 to 300 K. Mittal and Chaplot [21] calculated the density of states using semi-empirical interatomic potentials and generated the heat capacity from them. Yamamura *et al*. [22] used adiabatic scanning calorimetry to measure the heat capacity in the vicinity of the order–disorder (α –β) transition above 340 K.

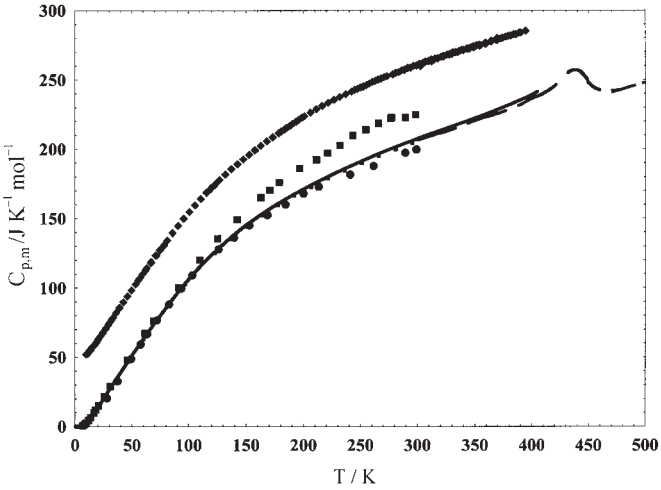

Fig. 1 Heat capacities of α-ZrW_2O_8 and β-$ZrMo_2O_8$ obtained on the high temperature calorimeter and comparison of the heat capacities reported for α-ZrW_2O_8 with those reported in the literature. Results for α-ZrW_2O_8: — BYU $C_{p,m}$; – – – Yamamura *et al*. [22]; • – Mittal and Chaplot [21]; ■ – Ramirez and Kowach [4]; • – BYU $C_{V,m}$ results. Results for β-$ZrMo_2O_8$: ◆ – shifted upward by 50 J K^{-1} mol^{-1}

The Ramirez and Kowach results [4] are consistently higher than those reported here, with the deviations increasing dramatically at T>100 K. They are also considerably higher than those reported by Yamamura *et al.* [22]. Agreement between the BYU and Yamamura results is quite good. The agreement between the BYU measurements and those obtained from the density of states calculation is good, although still not excellent above 200 K, even when $C_{p,m}$ has been corrected to $C_{V,m}$ using isothermal compressiblity and coefficients of thermal expansion from the literature [7, 23].

The experimental heat capacity of β-$ZrMo_2O_8$ is also shown in Fig. 1, shifted upward by 50 J K^{-1} mol^{-1}. No literature results are available for comparison. The molybdate is reported to adopt the disordered β-structure over the entire temperature range [9], however, there is some indication [10] that with slow cooling, ordering may take place below room temperature. We did not find any indication of a conversion throughout the time period of our measurements.

Chambers [24] has shown that plots of C/T^3 *vs*. ln(T/K) yield a representation of $1/\omega^2$ $G(\omega)$ *vs*. ln(ω) where ω is the energy and $G(\omega)$ is the density of vibrational states. In the Debye model, the density of states is quadratic in ω. A plot of a Debye heat capacity has a constant value up to $\ln(\omega)=\ln(\omega_D)$ where ω_D is the Debye frequency, and then decreases to 0 since $G(\omega)=0$ for $\omega>\omega_D$. In the temperature region, $T<\theta_D$, the magnitude of C/T^3 is inversely proportional to θ_D^3. Thus, a low energy Debye mode has a higher limiting value of C/T^3 than do high energy Debye modes. An Einstein mode is represented by a delta function in $G(\omega)$. $G(\omega)=\delta(\omega-\omega_E)=0$ for $\omega\neq\omega_E$ and is non-zero only for $\omega=\omega_E$. An Einstein mode appears in a C/T^3 plot as a symmetrical peak with a maximum at a temperature $T=\theta_E/4.93$. (Debye and Einstein temperatures, θ_D and θ_E, respectively, are related to frequencies by $\theta_i=h\omega_i/k_B$ for ω_i in Hz and $\theta_i=1.4388\ K\omega_i$ for frequencies expressed in wavenumbers, cm^{-1}.)

The characteristic features of the heat capacity, when plotted as C/T^3 *vs*. ln(T/K), are illustrated in Fig. 2a for θ_D=5, 50 and 100 K, and for θ_E = 5, 50 and 100 K in Fig. 2b. Because of the strong drop-off in the limiting values of C/T^3 as θ_D and in its maximum value as θ_E increases, curves with both θ_D and θ_E = 50 and 100 K are plotted on the smaller right-hand scale.

Table 1 Fitting parameters for the negative thermal expansion materials

Mode	α-ZrW_2O_8				β-$ZrMo_2O_8$	
	This study		Ramirez and Kowach [4]			
	n	θ/K	*n*	θ/K	*n*	θ/K
Debye 1	4.5e-5	3.38	0.008	20	–	–
Debye 2	10.25	220	22.5	650	8.52	214
Einstein 1	0.45	37.2	0.44	38.3	1.86	61
Einstein 2	1.55	62.2	1.7	58.0	–	–
Einstein 3	14.7	503	6.9	139.2	15.8	442

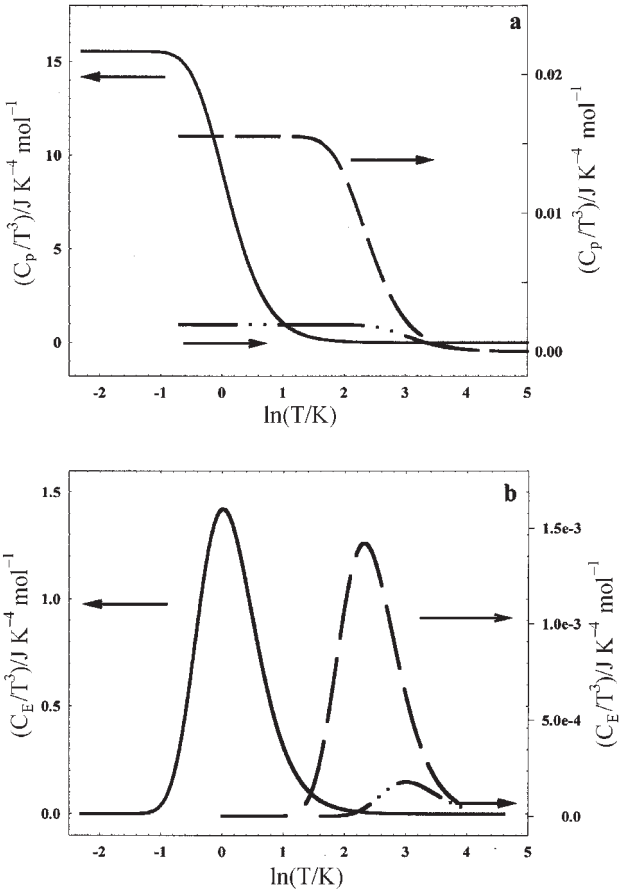

Fig. 2 Plots of C/T^3 *vs*. ln(T/K). a – Debye functions: — θ_D=5 K; – – θ_D=50 K; –··–·· θ_D=100 K; b – Einstein functions: — θ_E=5 K; – – θ_E=50 K; –··–·· θ_E=100 K

We follow the lead of Ramirez and Kowach [4] and analyze our experimental heat capacity results for ZrW_2O_8 and $ZrMo_2O_8$ using this format. The graphs are shown in Figs. 3a and 3b, respectively. Plots for the heat capacity of WO_3 and MoO_3 are shown for comparison in Fig. 3c. In these latter three compounds, results are available only from the high temperature apparatus. The two binary oxides show a small hump near 23 K that can be approximated as arising from a θ_E of 110 K. The NTE materials show larger maxima centered near $T\approx$10 K. The magnitude and location of the maxima indicate that the vibrational modes associated with these features are significantly lower in energy than those found in the binary oxides.

We can be more quantitative by fitting a series of Debye and Einstein functions to the experimental results using C/T^3 *vs*. ln(T/K) rather than the conventional C *vs*. T. The best fits, obtained using experimental results below 200 K, are shown in

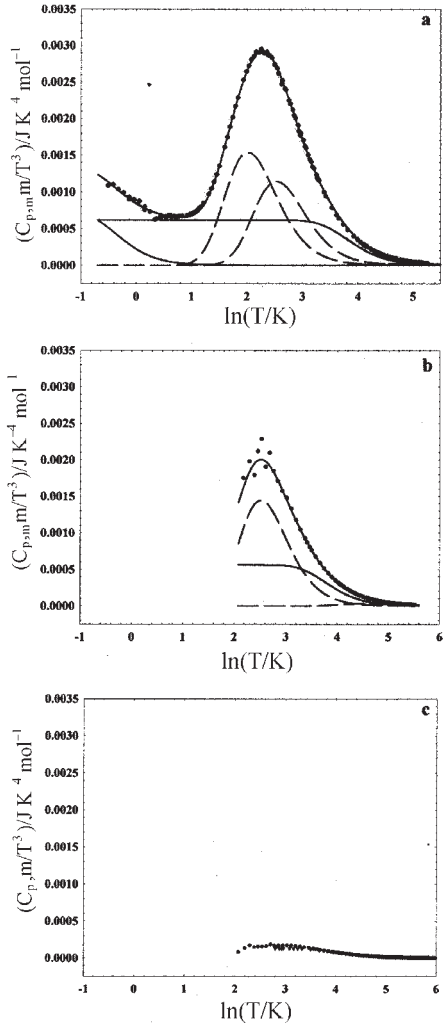

Fig. 3 Plots of C/T^3 *vs.* ln(T/K) for a – α-ZrW_2O_8; b – β-$ZrMo_2O_8$; and c – binary oxidies. For plots a and b, the following have been used: • – experimental points; solid lines are Debye functions; dashed lines are Einstein functions. Fitting parameters are in Table 1. For plot c only experimental points are shown: • – WO_3; ≻ – MoO_3

Figs 3a and 3b with solid lines representing Debye functions and dashed lines representing Einstein functions. The solid line through the experimental points is the sum of the contributions. The fitting parameters are given in Table 1.

Measurements of the very low temperature heat capacity of the molybdate will be reported elsewhere. Lacking this data, we are unable to be as quantitative with our

estimation of the very lowest modes in $ZrMo_2O_8$. However, a model with one fewer Debye and Einstein modes (eliminating the lowest ones from the ZrW_2O_8 fit) gives very good agreement to the available data.

Our fitting procedure differs from that employed by Ramirez and Kowach [4]. They fit functions to a data set that included measurements up to 300 K, and they appear to have constrained the sum of the weighting functions (*n*'s in our table, oscillator strengths in theirs) to total the vibrational degrees of freedom in the crystal (33/formula unit). We have chosen to include data only to 200 K in our fits. We do this both for reasons specific to the tungstate and molybdate materials and because of general characteristics of the data set expressed as C/T^3. In the tungstate and molybdate, there is an onset of the disorder transition and/or increased oxygen mobility [7, 25]. Restricting the data sets to results below 200 K prevents distortion of the fit by factors other than vibrational modes. This precludes our ability to observe high frequency modes that only contribute to the heat capacity at higher temperatures. However, since C/T^3 goes to 0 as temperature increases, good fits with high energy Debye and Einstein functions would not be obtained in any case. By leaving the weighting functions unconstrained, we allow for the existence of higher frequency modes. Still, our agreement with the results of the 2 Debye/3 Einstein fit of Ramirez and Kowach is relatively good, as shown in Table 1.

The most significant difference observed between the two sets of fits is that we require a very low temperature Debye (θ_D=3 K) function with a small weighting factor to reproduce the experimental results at the lowest temperatures. Our data extends about 0.4 K lower than that of Ramirez and Kowach and shows a clear upturn in C/T^3 below $\ln(T/\mathrm{K})\approx 0.5$. Data in their Figs 3 and 4 also shows the beginnings of that upturn. However, given the few points in the upturn, these authors cannot fit either Debye or Einstein functions.

Pure silica zeolites

We have previously reported heat capacity measurements of four zeolitic polymorphs of SiO_2: BEA, MFI, FAU and MTT from $10<T/\mathrm{K}<400$ [16]. (These names use the codes adopted by the Structure Commission of the International Zeolite Association. Detailed structural information can be found at their web site [26].) In our earlier paper, we reported that a fit using single Debye and Einstein frequencies could not adequately represent the heat capacity in the region from $20<T/\mathrm{K}<100$; calculated values were consistently low. However, the missing heat capacity could be well-represented by a Schottky function with energy gap of about 90 K.

To probe the possible source of such a contribution, we made measurements from $0.6<T/\mathrm{K}<100$ on two of the polymorphs, BEA and MFI. The samples were the same as those used previously [16], except that they have been recalcined at T=425 K to ensure that any residual carbon was removed. X-ray diffraction patterns of the powders before and after the heating were identical. Plots of these results in the form of C/T^3 *vs*. $\ln(T/\mathrm{K})$ are shown in Figs 4a and 4b.

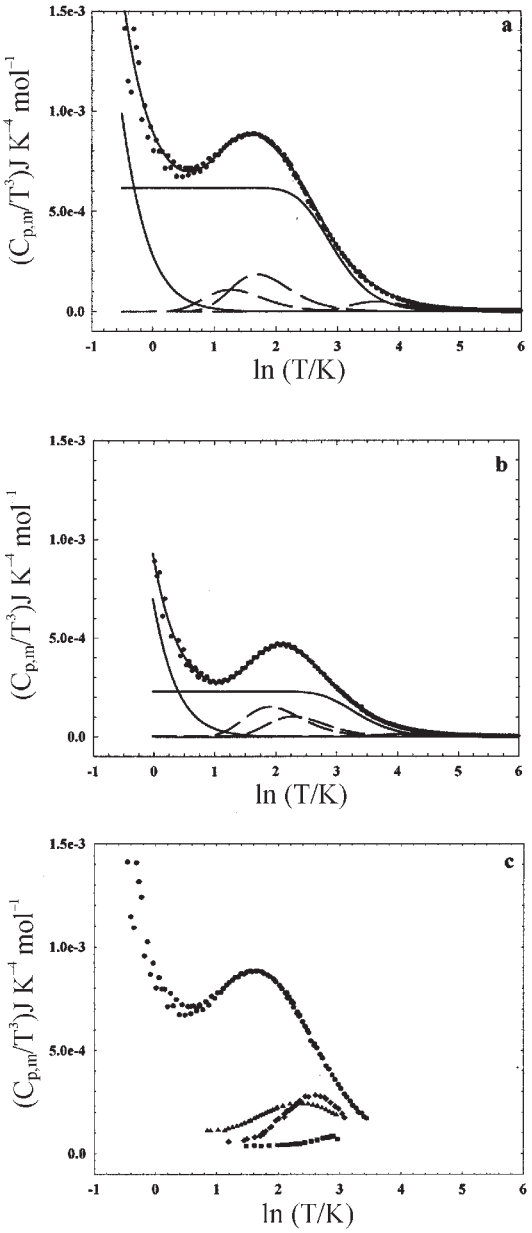

Fig. 4 Plots of C/T^3 *vs.* ln (T/K) for polymorphs of SiO_2. a – BEA; b – MFI; and c – dense SiO_2 phases. The following have been used in plots a and b: ● – experimental points; solid lines are Debye functions; dashed lines are Einstein functions. Fitting parameters are in Table 1. For plot c: ● – BEA; ▲ – quartz; ■ – vitreous silica; ◆ – cristobalite. The data for the dense phases of SiO_2 have been provided by Richet [29]

Table 2 Fitting parameters for the zeolitic polymorphs of SiO_2

Mode	BEA		MFI	
	n	θ/K	*n*	θ/K
Debye 1	3.9e-5	1.8	1.0e-4	2.3
Debye 2	0.600	85.7	0.730	128
Einstein 1	0.003	17.6	0.030	33.2
Einstein 2	0.021	26.9	0.066	48.6
Einstein 3	1.75	186	1.94	290

As with the ZrW_2O_8 and $ZrMo_2O_8$, we have been able to fit a series of Debye and Einstein functions to the experimental heat capacities of BEA and MFI. The results are summarized in Table 2. Comparison of the numerical results for the two suggests that BEA is floppier than MFI. The structural details of the two polymorphs are consistent with this interpretation. The channels and largest cavities of BEA are characterized by rings containing 12 silicon atoms, while the largest ring size found in MFI has only 10 silicon atoms [26].

The resemblance of the peaks in Figs 4a and 4b to the Boson peak [27] in vitreous silica is striking. Heat capacity plots of α-quartz, cristobalite and vitreous silica are compared with BEA in Fig. 4c to illustrate the similarity. BEA and MFI show larger peaks at lower temperatures than do any of the dense phases of SiO_2, indicating the presence of modes with lower energies in the zeolitic forms than in any of the dense phases, including the amorphous phase. This is an important result that may shed light on the nature of the Boson peak, which has been a matter of much debate.

The Boson peak has been attributed to an excess of low energy phonon modes in glasses over that predicted by the Debye model. An excess relative to that calculated from a θ_D determined from the speed of sound is also seen in α-quartz, but it is smaller and at higher energies than that observed in glasses. The excess in quartz is attributed to a larger than expected number of low-lying transverse optic phonon modes. In glasses, where the lack of translational symmetry makes it appropriate to think of phonons only in the long-wavelength limit, it is not clear that the same explanation is viable. A recent study [17] suggests that the Boson peak is associated with very low energy excitations of a rocking motion localized on small groups of tetrahedra. Dove and co-workers [28] have proposed a model that invokes vibrations of rigid tetrahedra about their flexible linkages. These Rigid Unit Modes (RUMs) have zero or very low energies. Molecular simulations based on this model predict localized vibrations in both glasses and zeolites [28]. Our experimental results on crystalline materials provide evidence for the existence of lower energy vibrations than have been observed in amorphous materials and may be associated with these localized excitations which can exist in either crystalline or amorphous materials.

Conclusions

Experimental heat capacities of α-ZrW_2O_8 and β-$ZrMo_2O_8$ and two polymorphs of SiO_2, BEA and MFI, have been modeled using Debye and Einstein functions with fitting calculations based on C/T^3 *vs*. $\ln(T/\mathrm{K})$. Debye and Einstein contributions with very low frequencies are required to reproduce the experimental results precisely. The lowest Debye energy in each case is unusually small and may be related to the RUM modes of Dove *et al*. [28] predicted in modelling studies of framework materials.

Low energy modes have been observed previously in ZrW_2O_8 and been related to NTE behavior in this material. Our measurements confirm their existence in the cubic molybdate. The frequencies extracted from the BEA and MFI heat capacities are lower than those found in dense phases of SiO_2 including the Boson peaks in vitreous silica. The existence of such modes in these zeolitic polymorphs is amenable with models that invoke localized excitations that could be present in either crystalline or amorphous materials. To the extent that the existence of low energy modes may be required for NTE behavior, it is proposed that MFE and BEA may be possible candidates for the existence of an NTE regime.

References

1 E. S. R. Gopal, Specific Heats at Low Temperatures, Plenum Press, New York 1966.
2 T. A. Mary, J. S. O. Evans, T. Vogt and A. W. Sleight, Science, 272 (1996) 90.
3 A. K. Pryde, K. D. Hammons, M. T. Dove, V. Heine, J. D. Gale and M. C. Warren, J. Phys. Condens. Matter, 8 (1996) 10973.
4 A. P. Ramirez and G. R. Kowach, Phys. Rev. Lett., 80 (1998) 4903.
5 G. Ernst, C. Broholm, G. R. Kowach and A. P. Ramirez, Nature (London), 396 (1998) 147.
6 W. I. F. David, J. S. O. Evans and A. W. Sleight, Europhys. Lett., 46 (1999) 661.
7 J. S. O. Evans, W. I. F. David and A. W. Sleight, Acta Cryst., B55 (1999) 333.
8 K. Wang and R. R. Reeber, Appl. Phys. Lett., 76 (2000) 2203.
9 C. Lind, A. P. Wilkinson, Z. Hu, S. Short and J. D. Jorgensen, Chem. Mater., 10 (1998) 2335.
10 J. S. O. Evans, P. A. Hanson, R. M. Ibberson, N. Duan, U. Kameswari and A. W. Sleight, J. Am. Chem. Soc., 122 (2000) 8694.
11 P. Tschaufeser and S. C. Parker, J. Phys. Chem., 99 (1999) 10609.
12 M. P. Attfield and A. W. Sleight, Chem. Commun., (1998) 601.
13 D. Woodcock, P. Lightfoot, L. A. Villaescusa, M.-J. Díaz-Cabañas, M. A. Camblor and D. Enberg, Chem. Mater., 11 (1999) 2508.
14 L. A. Villaescusa, P. Lightfoot, S. J. Teat and R. E. Morris, J. Am. Chem. Soc., 123 (2001) 5453.
15 S. H. Park, R. W. Grosse-Kunstleve, H. Graetsch and H. Gies, Stud. Surf. Sci. Catal., 105 (1997) 1989.
16 P. M. Piccione, B. F. Woodfield, J. Boerio-Goates, A. Navrotsky and M. E. Davis, J. Phys. Chem. B, 105 (2001) 6025.
17 E. Courtens, M. Foret, B. Hehlen and R. Vacher, Solid State Commun., 117 (2001) 187.

18 B. F. Woodfield, 'Specific Heat of High-Temperature Superconductors: Apparatus and Measurement.' Ph.D. Dissertation, Department of Chemistry, University of California, Berkeley, 1995.
19 B. F. Woodfield, J. Boerio-Goates, J. L. Shapiro, R. L. Putnam and A. Navrotsky, J. Chem. Thermodyn., 31 (1999) 245.
20 C. Lind, D. G. VanDerveer, A. P. Wilkinson, J. Chen, M. T. Vaughan and D. J. Weidner, Chem. Mater., 13 (2001) 487.
21 R. Mittal and S. L. Chaplot, Solid State Commun., 115 (2000) 319.
22 Y. Yamamura, N. Nakajima and T. Tsuji, Solid State Commun., 114 (2000) 453.
23 J. D. Jorgensen, Z. Hu, S. Teslic, D. N. Argyriou, S. Short, J. S. O. Evans and A. W. Sleight, Phys. Rev. B., 59 (1999) 215.
24 R. G. Chambers, Proc. Phys. Soc., 78 (1961) 941.
25 J. S. O. H. Evans, P. A. Ibberson, R. M. Duan, N. Kameswari and U. Sleight, J. Am. Chem. Soc., 122 (2000) 8694.
26 http://www.iza-structure.org/databases/
27 R. C. Zeller and O. Pohl, Phys. Rev. B, 4 (1971) 2029.
28 M. T. Dove, In: Reviews in Mineralogy and Geochemistry; S. A. T., Redfern, M. A., Carpenter, Eds, Mineralogical Society of America: Washington, DC 2000 Vol. 39, p 15.
29 Unpublished data at low temperatures for the dense phases of quartz has been provided by Dr. Pascal Richet, Laboratoire de Physique du Globe, 4 Place Jussieu, 75252 Paris Cedex 05, France.